MICROTEXTURES AND GEOCHEMISTRY OF GLASS AND CLAST LITHOLOGIES OF IMPACT-MELT FROM LONAR CRATER, INDIA.

S. Ghosh (sambhunath@prl.res.in) and D. Ray (dwijesh@prl.res.in)
PLANEX, Physical Research Laboratory, Ahmedabad 380 009, India

Introduction: The ~ 570 ka old Lonar crater, emplaced into the ~65 Ma old Deccan continental flood basalts of India, is one of the few well known impact craters on basaltic target [1, 2]. In addition to suevite breccias, shock induced Lonar glass mostly include impact-melt bomb and spherules which are sporadically recovered from the ejecta ~ 500m away from the crater rim [3, 6]. Earlier studies on Lonar impact-melt suggested geochemical similarity with the target basalts except characteristic depletion of Na_2O and enrichment of K_2O [3,4]. Present study reports a variety of microtextures and phase compositions related to different components of melt lithology and clast lithology of the Lonar shock glass to understand the chemical processes during shock melting.

Sampling and analytical techniques: Fresh pitch-black, vitreous lustered shock glass samples are selected from suevitic breccias of Lonar crater. A Cameca SX 100 electron microprobe has been used for analyses of major oxides. Quantitative major element analyses are performed at 15 kV accelerating voltage, 20 nA sample current, 1µm beam with routine PAP corrections and using natural mineral standards for calibration.

Microtextures of Shock glass: The glass is predominantly yellow to pale brown (under PPL) and often associated with vesiculated dark brown glass (Fig. 1). Backscattered electron (BSE) images reveal a matrix of smooth-textutred impure feldspathic glass and its devitrified products, acicular crystallites and feldspar microlites; latter being commonly nucleated at margins of anhedral to subhedral feldspar clasts (Figs. 2, 3). Other air- blown mineral clasts within the glassy matrix include euhedral to anhedral pyroxene (both low- and high Ca variety), Fe-Ti oxides besides rare occurrences of high- silica clasts and lithic clasts of the two- pyroxene target basalt (Fig. 4). Schlierens of titaniferous magnetite particles show swirling trails and laminar contortions around clasts suggesting flow texture of the impact melt (Fig. 3).

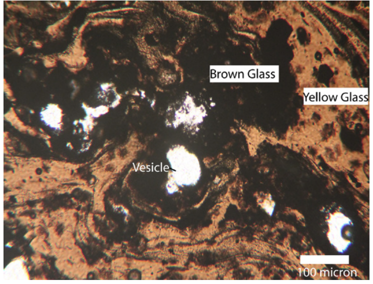

Fig. 1 Plane polarized (PPL) view of Lonar shock glass (yellow and dark brown colored) with flow texture. Note vesiculation in dark brown glass

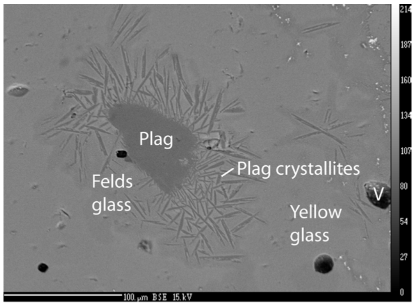

Fig. 2 BSE image of devitrification texture. Plagioclase (Plag) crystallites mark the nucleation sites around plag clast in the yellow glass.

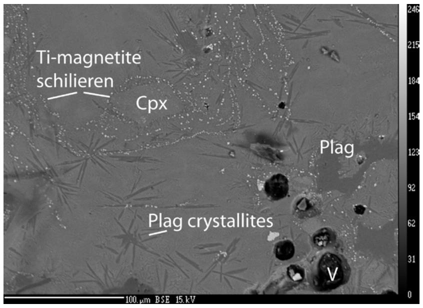

Fig. 3 BSE image of flow texture defined by Ti- magnetite schlieren within yellow glass. Mineral clast of clinopyroxene (Cpx) also seen.

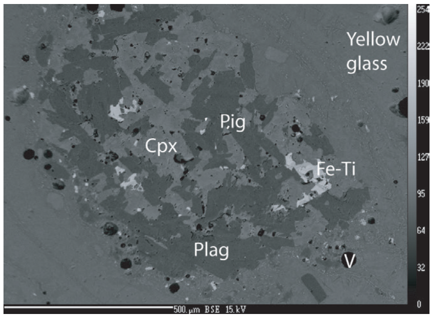

Fig. 4 BSE image of vesiculated lithic clast (Plagioclase, Clinopyroxene, Pigeonite (Pig) and Fe-Ti oxides) within the yellow glass

Geochemistry: Average Lonar impact glass composition is plotted in a spidergram after normalization against the average target basalt (Fig. 5, Table 1) and shows that the average composition of yellow glass partially deviates from target basalt in respect of Si, Mg and Ca and partially deviates from feldspathic glass, being depleted in Si, Al, Ca, Na and enriched in Fe, Mg, K and Ti. Compositionally dark brown glass is the hydrated variant of yellow glass only.

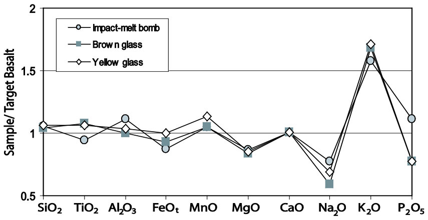

Fig. 5 Spidergram (normalized to target basalt) of yellow and brown glass and impact-melt bomb

Feldspar, the most abundant mineral clast within shock glass shows a large compositional variation ($An_{52-63}Ab_{35.5-45.5}Or_{1.5-2.7}$) and it corroborates with the plagioclase of lithic clast ($An_{41-62}Ab_{37-55}Or_{1.26-6.01}$).

By contrast, plagioclase crystallites and microlites are marginally enriched in MgO (1.2-1.6 wt%), FeO (3-5 wt%) and TiO_2 (0.5-0.7 wt%). Clinopyroxene clasts (Augite: $Wo_{26.5-37.3}En_{28.8-47.0}Fs_{18.8-39.9}$; Fe- pigeonite: $Wo_{10.5-11.4}En_{39.8-46.3}Fs_{43.3-48.8}$) are also compositionally similar with lithic clast pyroxenes (Augite: $Wo_{35-38}En_{39-41}Fs_{20-26}$; Fe- pigeonites:$Wo_{10-15}En_{34-35}Fs_{45-51}$). Some pigeonites with corroded / diffuse margins show marginal enrichment of SiO_2 (56-58 wt%), substantially enriched Al_2O_3 (10 wt%), sub calcic (Wo <20 mol%) and nonstoichiometric composition. Fe-Ti oxides within the shock- glass show generally two clusters (FeO: 66 wt%; TiO_2: 26 wt% and FeO: 82 wt%; TiO_2: 9-11 wt%). Exsolved ilmenites are locally noted within the titanomagnetite host of lithic clast. In contrast to mineral clasts, Si-rich clasts (SiO_2~ 75-85 wt%; Al_2O_3~ 12-15 wt%; CaO~ 1.2-3.8 wt%, K_2O~ 0.2-2.4 wt%) are locally present in the yellow glass. Rarely noticed vesiculated silica clasts (SiO_2 ~96 wt%) seem to represent the weathered topmost horizon of target basalt.

Table 1 Average bulk chemical compositions of target basalt, impact-melt bomb and glass (yellow and brown glass)

	Lonar target basalt[3] (16)	Impact-melt-bomb[3] (7)	Yellow Glass (33)	Brown Glass (11)
SiO_2 (wt%)	47.82	50.15	50.49	49.92
TiO_2	2.26	2.26	2.35	2.44
Al_2O_3	12.96	13.52	13.52	12.93
FeO_t	14.22	13.85	13.89	13.26
MnO	0.19	0.21	0.21	0.20
MgO	6.07	5.67	5.18	5.10
CaO	9.87	9.47	9.98	9.92
Na_2O	3	1.98	2.14	1.77
K_2O	0.38	0.67	0.61	0.64
P_2O_5	0.27	0.30	0.22	0.21
Total	97.04	98.08	98.6	96.39
Mg#	0.43	0.42	0.40	0.41
CIPW norm				
Quartz	5.19	2.06	2.07	4.32
Orthoclase	2.25	3.55	3.60	3.78
Albite	25.39	19.63	18.11	14.98
Anorthite	20.77	27.05	25.48	25.44
Diopside	15.02	16.99	19.03	18.84
Hypersthene	8.15	24.19	25.32	23.90
Ilmenite	0.4	4.06	4.46	4.63
Apatite	0.64	0.71	0.52	0.50

Mg# moleMg/mole(Mg+Fe)

Discussion: Aerodynamic shape of the impact glass bomb and flow structure within the impact glass suggest they were in molten state during the time of atmospheric flight. Development of feldspar crystallites and microlites account for quenching and devitrification of the melt. Nucleation of crystallites / microlites is more conducive at the contact of mineral clasts, as indicated in feathery appearance at the plagioclase rim. Metastable phases of corroded low-Ca pigeonite clast and tiny particles/ droplets of Fe-Ti oxides represent the impact-caused destabilised products after contribution of Fe-Mg cations and Ti-Fe cations respectively in the yellow glass. Escape of volatiles under high confining pressure causes profuse vesiculation in the glass. Textural evidences suggest yellow glass is similar to Class 5 shock glass (> 80 GPa, [4]). Overlapping geochemistry of the shock glass with that of the target rock refers to quartz- normative tholeiite basalt as its precursor. Ternary plagioclase with higher normative anorthite (25.5%) and orthoclase (3.6%) content suggests plagioclase dominated melting. This is also reflected in the geochemistry of impact melt-bomb and mm- to submillimeter spherules [3,5,6,7,8]. Destabilisation of Fe-Ti spinel clasts, indicated from schilieren texture, is responsible for marginal Ti- enrichment in yellow shock glass with concomittant depletion of Ti and minor enrichment of SiO_2, MgO and Al_2O_3 in trails of quenched titaniferous magnetite particles / droplets.

Compositional continuity between quenched yellow shock glass (melt phase) and coexisting plagioclase microlites (solid phase) suggests the two inequilibrium fractions of a secondary precursor generated by impact from primary precursor (target basalt). Secondary precursor is a plagioclase-dominated melt with incorporation of Fe^{2+}, Mg^{2+} cations from destabilized pigeonite and Ti^{4+}, Fe^{2+} cations from metastable Fe-Ti oxides in different proportions. It is envisaged that crystal fractionation of the Lonar tholeiitic magma might have produced immisciblity between Fe- rich basaltic liquid and Si- rich pegmatitic liquid [9]; the latter being represented locally as silica-rich clast. Finally, chemical processes of Lonar impact melt could be considered in ideal mimic to impact melt of basaltic shergottite.

References: [1] Fredriksson K. et al. (1973) *Science*, *180*, 862-864. [2] Jourdon F. et al. (2011) *Geology*, *39*, 671-674. [3] Osae S. et al. (2005) *MAPS*, *40*, 1473-1492. [4] Keiffer S.W. et al. (1976) Proc. 7th Lunar Sci Conf., 1391-1412 [5] Son T.H. & Koeberl C. (2007) *GFF*, *129*, 161-176. [6] Ghosh S. and Bhaduri S. (2004) *Ind. Min.*, *57*, 1-26. [7] Misra S. et al. (2009) *MAPS*, *44*, 1001-1018. [8] Ray D. et al. (2013) 44th LPSC, abstract no 1031. [9] Lofgren G.E. (1977) Porc. 8th Lunar Sci. Conf., 2079-2095.